

## Combustion process in a spark ignition engine: Dynamics and noise level estimation

T. Kamiński and M. Wendeker

*Department of Combustion Engines, Technical University of Lublin, Nadbystrzycka 36, PL-20-618 Lublin, Poland*

K. Urbanowicz

*Faculty of Physics, Warsaw University of Technology, Koszykowa 75, PL-00-662 Warsaw, Poland*

G. Litak<sup>a)</sup>

*Department of Mechanics, Technical University of Lublin, Nadbystrzycka 36, 20-618 Lublin, Poland*

(Received 8 October 2003; accepted 19 March 2004; published online 21 May 2004)

We analyze the experimental time series of internal pressure in a four cylinder spark ignition engine. In our experiment, performed for different spark advance angles, apart from the usual cyclic changes of engine pressure we observed additional oscillations. These oscillations are with longer time scales ranging from one to several hundred engine cycles depending on engine working conditions. Based on the pressure time dependence we have calculated the heat released per combustion cycle. Using the time series of heat release to calculate the correlation coarse-grained entropy we estimated the noise level for internal combustion process. Our results show that for a larger spark advance angle the system is more deterministic. © 2004 American Institute of Physics.

[DOI: 10.1063/1.1739011]

**Combustion process in spark ignition engines is widely known as a nonlinear and noisy process. Instabilities, which are occurring as cycle-to-cycle variations of internal cylinder pressure, effect directly the power output. Examination of these variations can lead to better understanding of their sources and help in their elimination in a future engine control procedure. Improving engine efficiency requires achieving better combustion conditions without introducing additional disturbances. In the present paper we analyze the dynamics of a combustion process and we estimate the noise level based on experimental time series of internal pressure and calculated from them heat release. In the following analysis we apply the nonlinear multidimensional methods which can distinguish random variations from a deterministic behavior.**

### I. INTRODUCTION

Combustion in four stroke spark ignition (SI) engines is a complex cyclic process consisting of air intake, fuel injection, compression, spark ignition, combustion, expansion, and finally gas exhaust phases (Fig. 1) where burned fuel power is transmitted through the piston to the crankshaft. In the beginning of SI engine development there were observed instabilities of combustion.<sup>1</sup> These instabilities cause fluctuations of the power output making it difficult to control.<sup>2,3</sup> The problems of their source identification and their elimination have become main issues in SI engine technologies engineering, which have not been solved up to the present time.<sup>4</sup> Among the main factors of instabilities classified by

Heywood<sup>5</sup> are aerodynamics in the cylinder during combustion, amounts of fuel, air, and recycled exhaust gas supplied to the cylinder, and a local mixture composition near the spark plug.

Recently, Daw *et al.*<sup>6,7</sup> and Wendeker *et al.*<sup>8</sup> have done the nonlinear analysis of such process. Changing an advance spark angle they observed a considerable increase of pressure fluctuations level,<sup>8</sup> claiming that it is due to nonlinear dynamics of the process. In the other work,<sup>9</sup> Wendeker and co-workers proposed an intermittency mechanism to explain the route to chaotic combustion.

Prompted by these findings we decided to analyze the correlation entropy of the combustion process in different working conditions of the engine. With the help of the entropy produced by the dynamical system we can quantify the level of measurement or dynamical noise.<sup>10</sup> In the present paper we shall start our analysis by examining experimental pressure time series.

It should be noted that pressure is the best known quantity to analyze engine dynamics. Cylinder pressure together with volume data can be used to obtain indicated mean effective pressure, calculate the engine torque, indicated efficiency and also burn rate, bulk temperature and heat release. Moreover, statistical analysis of the pressure data can also provide information about combustion process stability.

However, in practice, it is not easy to perform direct measurement of pressure,<sup>11</sup> as one needs a good sensor persistent to high temperatures to be placed inside the engine cylinder. Therefore to obtain information about pressure some researchers developed alternative non-direct measurement procedures.<sup>12</sup>

In our particular case we have been dealing with well established piezo-electric sensors, which enabled us to mea-

<sup>a)</sup>Electronic mail: g.litak@pollub.pl

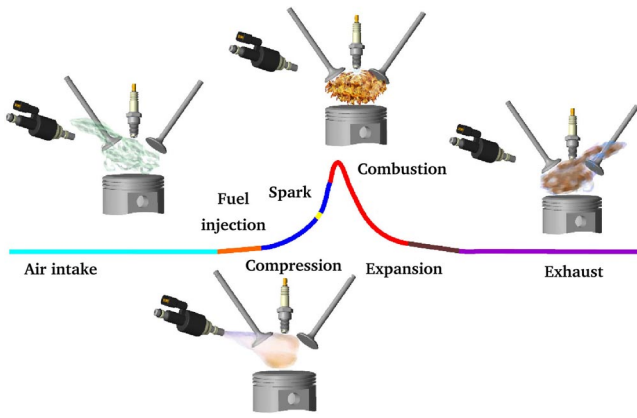


FIG. 1. (Color online) A schematic picture of a typical combustion cycle in a four stroke spark ignition engine.

sure pressure directly to examine the dynamics of combustion more effectively.<sup>8,9</sup>

The present paper is divided into six sections. After a short introduction (Sec. I), we provide a description of our experimental standing and measurement procedure in Sec. II. There we show some examples of cycle-to-cycle variations in pressure inside one of the cylinders. In Sec. III, we examine the pressure in more detail. We will perform a spatiotemporal analysis comparing the fluctuations of pressure in succeeding cycles for different advance angles. In Sec. IV we calculate the heat release per cycle. Finally, in Sec. V we analyze its time dependence and show our main result, i.e., level of noise. We end up with conclusions and final remarks (Sec. VI).

## II. EXPERIMENTAL FACILITIES AND MEASUREMENTS OF INTERNAL PRESSURE

In our experimental stand (Fig. 2) pressure was measured directly inside the cylinder by the use of the piezoelectric sensor. Such equipment provides one of the most direct measures of combustion quality in an internal combustion engine. Internal pressure data were obtained from Engine Laboratory of Technical University of Lublin, where we conducted a series of tests.

The pressure traces were generated on a 1998 cm<sup>3</sup> Holden 2.0 MPFI engine at 1000 rpm. The data were captured using NUDAC-TK version 2.0 data acquisition and data processing program.<sup>13</sup> The original files contained cylinder pressure at crank angles 0°–720°. Each of three large files (about 990 Mbytes each) contained above 10 000 combustion cycles. Data were taken at different spark timings (spark advance angles): 5°, 15°, and 30° before top dead center. The engine speed, air/fuel ratio, and throttle setting were all held

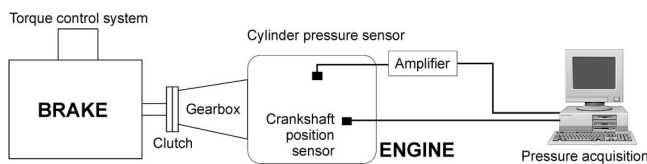


FIG. 2. Experimental stand.

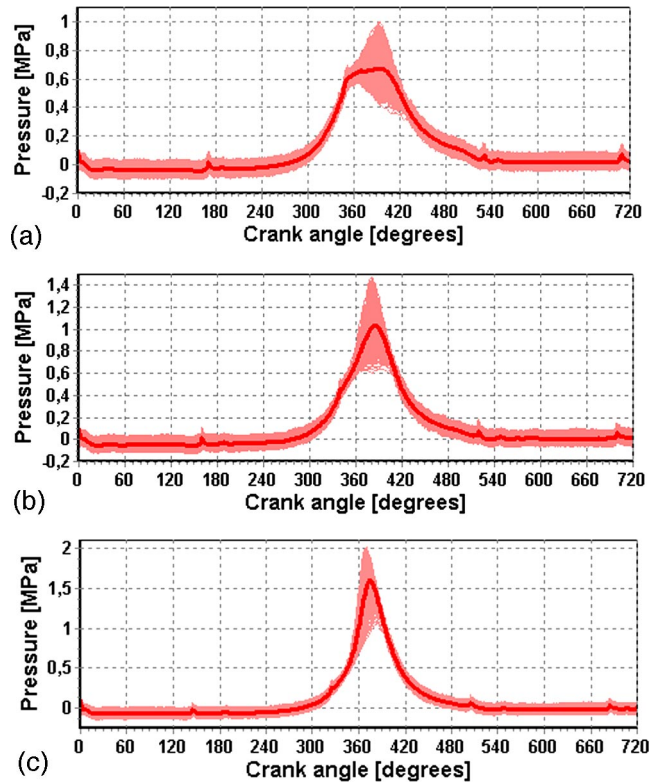


FIG. 3. (Color online) Internal pressure of 1000 combustion cycles against a crank angle for a spark advance angle  $\Delta\alpha_z = 5^\circ$ ,  $15^\circ$  and  $30^\circ$  for (a), (b), and (c), respectively. Full lines correspond to the average angular pressure.

constant throughout the data collection period. Intake air pressure, in inlet pipe, had a value of 40 kPa. The torque for each of three spark timings were adequate: 21, 28, and 30 N m.

To perform signal analysis we needed sufficiently large experimental data. In this aim we measured 10 000 cycles for each of the three spark advance angles  $\Delta\alpha_z$ . The results for the first 1000 cycles are shown in Figs. 3(a)–3(c). Note that depending on an advance angle we have more or less broadened the region of pressure fluctuations. The full line shows the pressure averaged over the first 1000 cycles. It is increasing with growing  $\Delta\alpha_z$  and reaches its highest value for  $\Delta\alpha_z = 30^\circ$ .

Note also that in our four stroke engine the combustion period (Figs. 1 and 3) corresponds exactly to the double period of the crankshaft revolution synchronized with a single spark ignition. Every combustion cycle starts with initial conditions given by a mixture of air and fuel. All of the succeeding cycles are separated by gas exhaust and intake stroke phases. That process is in general nonlinear and can also be mediated by stochastic disturbances coming from, e.g., nonhomogeneous spatial distribution of fuel/air ratio. After combustion, exhaust gases are mixed with fresh portions of fuel and air.

Therefore the residual cylinder gases after each combustion cycle influence the process in a succeeding cycle leading to different initial conditions of air, fuel, and residual gas mixture contents.

TABLE I. Definitions of variables and symbols used.

Position of the piston	$h$
Internal cylinder pressure	$P$
Actual cylinder volume	$V(\alpha)$
Heaviside step function	$\Theta(z)$
Heat released	$Q$
Heat released in particular cycle $i$	$Q_i$
Heat released vector in embedding space	$\mathbf{Q}$
Spark advance angle	
$\Delta\alpha_z$ embedding time delay in cycles	$m$
Cycle number	$i, j$
Embedding dimension	$n$
Number of considered points in time series	$N$
Loading torque	$F$
Crank angle	$\alpha \in [0, 720^\circ]$
Threshold	$\varepsilon$
Correlation integral	$C^n$
Coarse-grained correlation integral	$C^n(\varepsilon)$
Correlation entropy	$K_2$
Coarse-grained correlation entropy	$K_2(\varepsilon)$
Calculated from time series	
Coarse-grained entropy	$K_{\text{noisy}}$
Correlation dimension	$D_2$
Noise-to-signal ratio	NTS
Standard deviation of data	$\sigma_{\text{data}}$
Error function	$\text{Erf}(z)$
Fitting parameters	$\chi, a, b$
Standard deviation of noise	$\sigma$
Cylinder diameter	$D = 86 \text{ mm}$
Crank radius	$r = 43 \text{ mm}$
Connecting-rod length	$l = 143 \text{ mm}$
Heating value of the fuel	$W_u = 43000 \text{ kJ/kg}$
Compression ratio	$\epsilon = 8.8$
Poisson constant	$\kappa = \frac{c_p}{c_v} \approx 1.4$
Mass burned in cycle $i$	$M_i$
Autocorrelation function	$AC(j)$
Output torque	$S$

III. ANALYSIS OF PRESSURE

During the combustion process the internal volume of the engine cylinder is driven kinematically by the piston. As a consequence of the above it also changes periodically as a function of crank angle  $\alpha$  and satisfies the relation

$$V(\alpha) = \pi \frac{D^2}{4} h + \pi \frac{D^2}{4} 2r \frac{1}{\epsilon - 1}, \tag{1}$$

where the piston position  $h$ ,

$$h = r(1 - \cos \alpha) + l \left( 1 - \frac{r}{l} \sqrt{\frac{l^2}{r^2} - \sin^2 \alpha} \right), \tag{2}$$

and constants  $r, l, D$  as well as  $\epsilon$  are defined in Table I.

In some sense the combustion initiated by ignition in each engine cycle is an independent combustion event. Such events are separated by the processes of exhaust and intake dependent on the amount of combusting fuel mass and quality of newly prepared fuel-air mixture. To illustrate this effect we show in Figs. 4(a)–4(c) spatiotemporal plots corresponding to the first 1000 cycles of our pressure time series for different advance angle  $\Delta\alpha_z = 5^\circ, 15^\circ, 30^\circ$ , respectively. Each color in Figs. 4(a)–4(c) corresponds to one of four intervals of  $[P_{\min}, P_{\max}]$ : white  $[P_{\min}, P_1]$ , light gray  $[P_1, P_2]$ , dark gray  $[P_2, P_3]$ , and black  $[P_3, P_{\max}]$ .

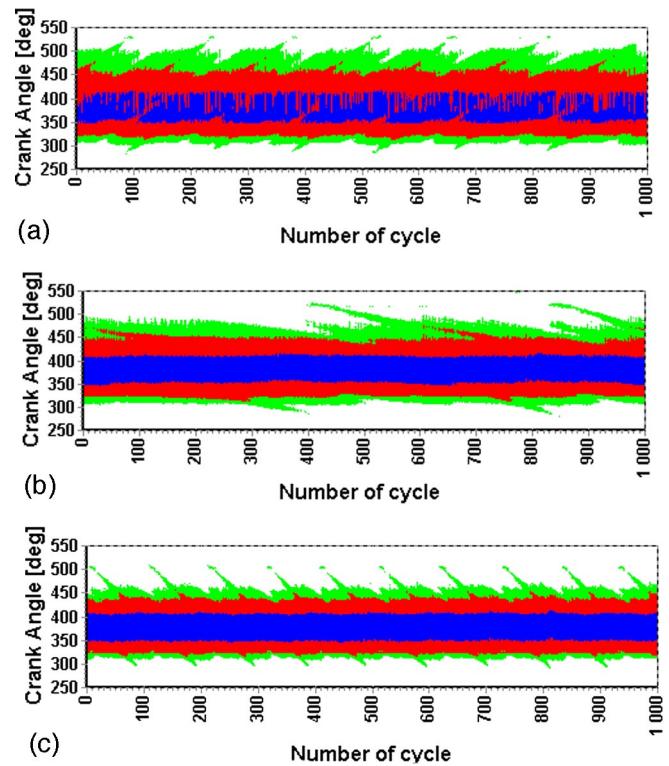


FIG. 4. (Color online) Four color spatiotemporal diagram corresponding combustion process with system parameters as in Figs. 3(a)–3(c), respectively. Each color corresponds to one of four intervals of  $[P_{\min}, P_{\max}]$ : white  $[P_{\min}, P_1]$ , light gray  $[P_1, P_2]$ , dark gray  $[P_2, P_3]$ , and black  $[P_3, P_{\max}]$  ( $P_{\min} = -0.2 \text{ MPa}$ ,  $P_1 = 0.1 \text{ MPa}$ ,  $P_2 = 0.2 \text{ MPa}$ ,  $P_3 = 0.6 \text{ MPa}$ ,  $P_{\max} = 2.0 \text{ MPa}$ ).

One can easily see that the pressure signal, especially in Fig. 4(c), seems to change in some regular manner of a time scale of about 100 cycles. A similar feature is also visible in Fig. 4(a) while it is difficult to find such regularity in Fig. 4(b). Note that the main difference in these three diagrams occurs in regions assigned to a green color, corresponding to relatively small pressure. However, the diagram Fig. 4(a) has an additional feature. In this case the broader angular interval of fluctuations visible in Fig. 3(a) has its consequence in the irregularly changing border between red and blue colors.

IV. VARIATIONS OF HEAT RELEASE

To capture the cycle-to-cycle changes in combustion process we decided to calculate of heat release in a sequence of combustion cycles. This quantity is more convenient to examine the stability of the combustion process because it enables us to concentrate on it. In contrast to that, internal pressure itself is simultaneously effected by combustion and by cyclic compression. It is also worth noticing that heat release also has practical meaning as it is proportional to burned fuel mass.

For an adiabatic process the heat released from chemical reactions during combustion in the engine is given by a differential equation, coming from the first law of thermodynamics, with respect to a crank angle  $\alpha$ ,

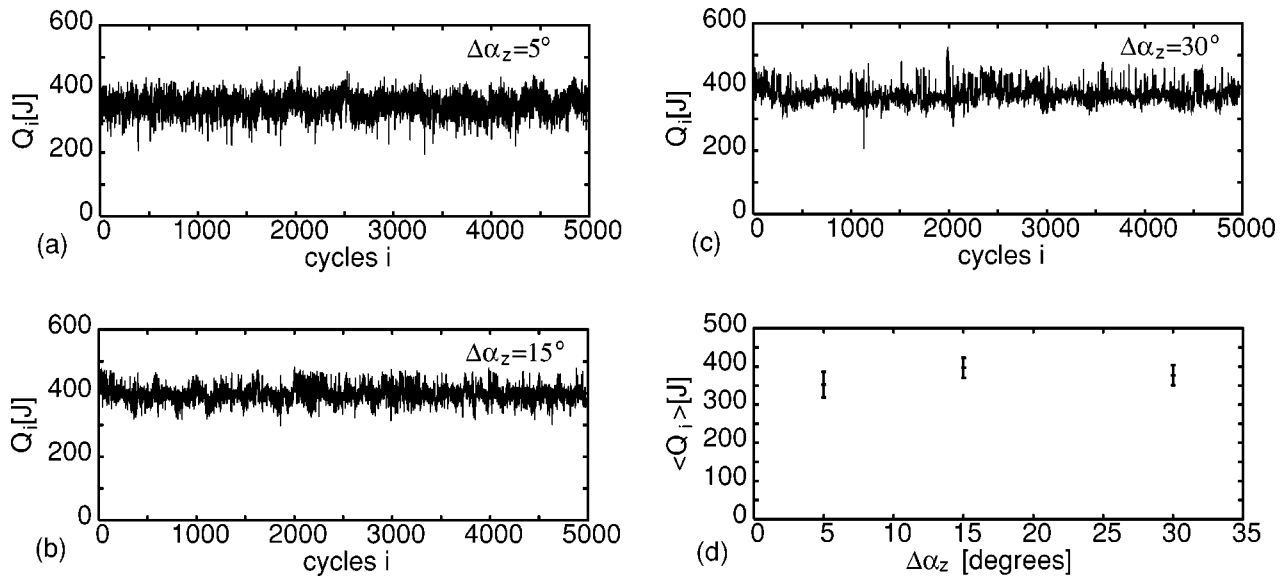


FIG. 5. Heat release per cycle  $Q_i$  vs sequential cycles  $i$  for a spark advance angle  $\Delta\alpha_z = 5^\circ$ ,  $15^\circ$ , and  $30^\circ$  for (a), (b), and (c), respectively. The average heat release vs an advance angle  $\Delta\alpha_z$ .

$$\frac{dQ}{d\alpha} = \frac{\kappa}{\kappa-1} P \frac{dV}{d\alpha} + \frac{1}{\kappa-1} V \frac{dp}{d\alpha}. \quad (3)$$

Using Eq. (3) together with the experimental pressure time series and parametric change of cylinder volume  $V$ , Eqs. (1) and (2), we have calculated the heat released in succeeding cycles  $Q_i$ .

It can be closely related to the burned fuel mass in one cycle  $M_i$ ,

$$M_i = Q_i / W_u, \quad (4)$$

where  $W_u$  is the heating value of the fuel, listed in Table I. It should be underlined that Eq. (4) neglects the effects of heat exchange between the cylinder chamber and its walls. This is in the spirit of an adiabatic process assumption [Eq. (3)]. Of course the consumed mass will be larger because it also depends on the quality of mixture and combustion process.

In Fig. 5, the calculated heat release  $Q_i$ , for the first 5000 cycles is plotted against cycles succeeding  $i$  [Figs. 5(a)–5(c) for  $\Delta\alpha_z = 5^\circ$ ,  $15^\circ$ ,  $30^\circ$ , respectively].

Note that in all examined cases there is some modulation ranges from one to a few hundred cycles. Interestingly, for small advance angles  $\delta\alpha_z = 5^\circ$  or  $15^\circ$  this modulation evolves indicating that the system can have quasi-periodic or chaotic nature. Note also for the first 1000 variations for  $\Delta\alpha_z = 5^\circ$  [Fig. 5(a)] resembles those for  $\Delta\alpha_z = 30^\circ$  [Fig. 5(c)], while for  $\Delta\alpha_z = 15^\circ$  the long time scale modulation is different. This is consistent with Figs. 4(a)–4(c). Generally, for  $\Delta\alpha_z = 30^\circ$  the oscillations are of higher frequency and more regular. In Fig. 5(d) we plotted the average value of  $\langle Q_i \rangle$ . ( $\langle Q_i \rangle = 352.54$  J—for  $\Delta\alpha_z = 5^\circ$ ,  $\langle Q_i \rangle = 396.67$  J—for  $\Delta\alpha_z = 15^\circ$  and  $\langle Q_i \rangle = 377.04$  J—for  $\Delta\alpha_z = 30^\circ$ ). Note that it is the largest for  $\Delta\alpha_z = 15^\circ$ , indicating the largest burning rate of fuel. On the other hand the output torque, for the same speed of a crankshaft, was changing from the largest

value  $S = 30$  Nm, in the case  $\Delta\alpha_z = 30^\circ$ , to slightly smaller and  $S = 28$  Nm for  $\Delta\alpha_z = 15^\circ$  and much smaller  $S = 21$  Nm for  $\Delta\alpha_z = 5^\circ$ .

The account for the fresh fuel rate was the same in all the cases and we conclude there are better combustion conditions for larger advance angles. Evidently, in the case of  $\Delta\alpha_z = 5^\circ$  some amount of fuel was not burned.

To further examine the nature of  $Q_i$  fluctuations we have calculated autocorrelation function from the whole 10 000 cycle signal via

$$AC(j) = \sum_i Q(i)Q(i+j) \quad (5)$$

with appropriate normalization to one. The results for all three advance angles  $\Delta\alpha_z$  are depicted in Figs. 6(a)–6(c) (for  $\Delta\alpha_z = 5^\circ$ ,  $15^\circ$  and  $30^\circ$ ). One can see that the decay rate of  $AC(j)$  amplitude with growing  $j$  is comparable for  $\Delta\alpha_z = 5^\circ$  and  $30^\circ$ , but differs fundamentally from the  $\Delta\alpha_z = 15^\circ$  case where it decays much faster. Note that this result corresponds to Fig. 4(b), where the period pressure time dependence was not presents contrast to Figs. 4(a) and 4(c). Higher value of an autocorrelation function is naturally associated with the appearance of additional longer scale oscillations of pressure.

## V. ESTIMATION OF NOISE LEVEL FROM HEAT RELEASE SERIES

Here we shall examine the level of noise in heat release time series. Toward this aim we use a nonlinear embedding space approach.<sup>14</sup>

In the  $n$  dimensional embedding space the state is represented by a vector

$$\mathbf{Q} = \{Q_i, Q_{i+m}, Q_{i+2m}, \dots, Q_{i+(n-1)m}\}, \quad (6)$$

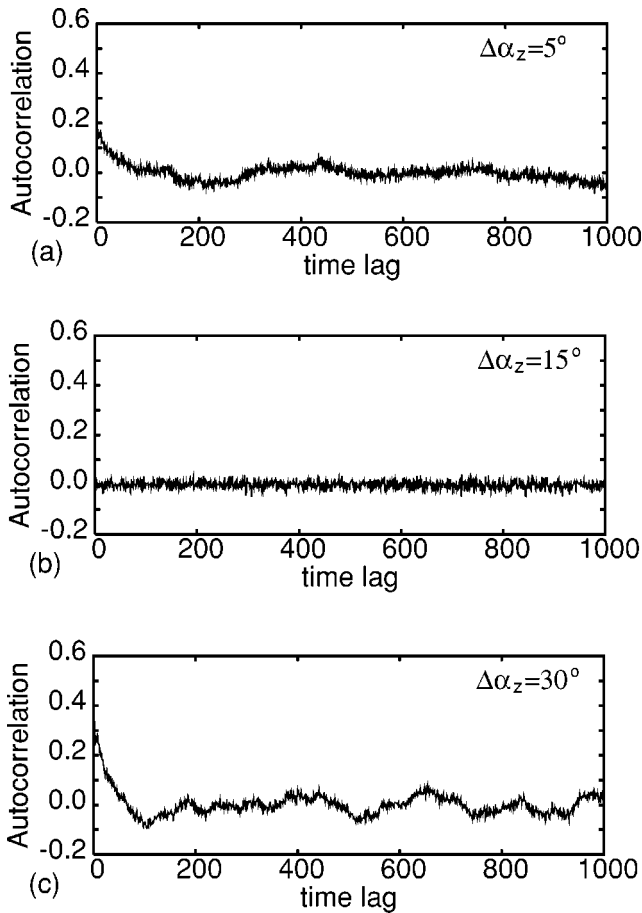


FIG. 6. The autocorrelation function calculated from heat release time series for different advance angles  $\Delta\alpha_z$ .

where  $m$  denotes the embedding delay in terms of cycles. The correlation integral calculated in the embedding space can be defined as<sup>15,16</sup>

$$C^n(\varepsilon) = \frac{1}{N^2} \sum_i^N \sum_{j \neq i}^N \Theta(\varepsilon - \|\mathbf{Q}_i - \mathbf{Q}_j\|), \quad (7)$$

where  $N$  is the number of considered points corresponding to pressure peaks in cycles and  $\Theta$  is the Heaviside step function. For simplicity we use maximum norm. The correlation integral  $C^n(\varepsilon)$  is related to the correlation entropy  $K_2(\varepsilon)$  and the system correlation dimension  $D_2$  by the following formula:<sup>15,16</sup>

$$\lim_{n \rightarrow \infty} C^n(\varepsilon) = D_2 \ln \varepsilon - nmK_2(\varepsilon). \quad (8)$$

The coarse-grained correlation entropy can be now be calculated as

$$K_2(\varepsilon) = \lim_{n \rightarrow \infty} \ln \frac{C^n(\varepsilon)}{C^{n+1}(\varepsilon)} \approx - \frac{d \ln C^n(\varepsilon)}{dn}. \quad (9)$$

In such a case the correlation entropy is defined in the limit of a small threshold  $\varepsilon$ .

In the presence of noise described by the standard deviation  $\sigma$  of  $\mathbf{Q}_i$  time series, the observed coarse-grained entropy  $K_{\text{noisy}}$  (Ref. 10) can be written as

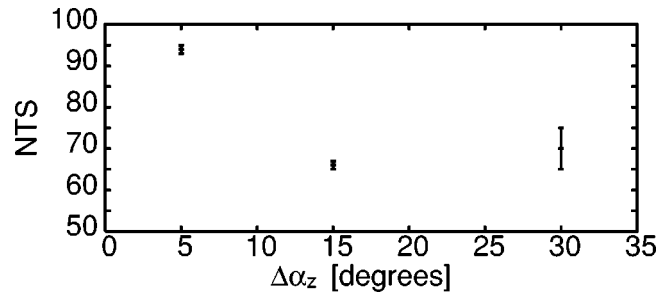


FIG. 7. The noise to signal ratio (NTS) vs a spark advance angle  $\Delta\alpha_z$ .

$$K_{\text{noisy}}(\varepsilon) = - \frac{1}{m} g\left(\frac{\varepsilon}{2\sigma}\right) \ln \varepsilon + [\chi + b \ln(1 - a\varepsilon)] \times \left(1 + \sqrt{\pi} \frac{\sqrt{\varepsilon^2/3 + 2\sigma^2 - \varepsilon/\sqrt{3}}}{\varepsilon}\right). \quad (10)$$

Function  $g(z)$ , present in the above-mentioned formula, reads

$$g(z) = \frac{2}{\pi} \frac{z e^{-z^2}}{\text{erf}(z)}, \quad (11)$$

where  $\text{erf}(\cdot)$  is the error function. The parameters  $\chi$ ,  $a$ ,  $b$  as well as  $\sigma$  are unconstrained. They should be fitted in Eq. (10) to mimic the observed noisy entropy calculated from available data.

After application of the above-noted method to the heat release time series we estimated noise calculating the noise to signal ratio (NTS):

$$\text{NTS} = \frac{\sigma}{\sigma_{\text{data}}}, \quad (12)$$

where  $\sigma_{\text{data}}$  is the standard deviation of data.

Figure 7 shows NTS versus a spark advance angle  $\Delta\alpha_z$ . It appeared that for any of the examined cases the noise level is high. Starting from a small spark advance angle  $\Delta\alpha_z = 5^\circ$  the level of noise is the highest  $\text{NTS} \approx 94\%$ . It diminishes to about 66% for  $\Delta\alpha_z = 15^\circ$  and slightly grows to 70% for  $\Delta\alpha_z = 30^\circ$ , respectively. These results together with behavior of an autocorrelation function [Figs. 6(a)–6(c)] indicate that for  $\Delta\alpha_z = 15^\circ$  combustion process is the most stable.

## VI. REMARKS AND CONCLUSIONS

In this paper we analyzed instabilities of a combustion process. At first we focused on nonlinear analysis of pressure time series. Using spatiotemporal methods we established that for some combustion conditions there is another unexpected long time scale in fluctuation of our experimental data. To examine this phenomenon in detail we calculated heat release and we performed the noise level estimation using nonlinear multidimensional methods. Our results clearly indicate that the noise in the time series is the highest for the smallest advance angle.

Heat released in cycle, as a practical parameter closely related to burned fuel mass, is capable of following the stability of the combustion process better than any other quan-

tity. Our noise estimation based on heat release time series is more credible than the analysis pressure histories themselves, as pressure is effected by volume cyclic compression and expansion phases.

Our results clearly indicate that stochastic noise level appeared to be the highest for a small advance angle  $\Delta\alpha_z$ . It diminished for larger  $\Delta\alpha_z$  stabilizing at about  $70^\circ$  for the optimal angle. This can be easily understood if one only recalls that the combustion process, lasting a few milliseconds, started too late and is finishing in conditions of a relatively large volume of combustion chamber. This results in partial combustion of an air/fuel mixture. Increasing an advance angle leads to a smaller combustion chamber volume and consequently improves the combustion efficiency. However, the angle  $\Delta\alpha_z=30^\circ$  seems to be too large. In such a case ignition starts too early in worse thermal condition, resulting in instabilities of a flame.

Interestingly, in cases of  $\Delta\alpha_z=5^\circ$  and  $30^\circ$  we have obtained the signal with characteristic 100 cycle periodicity [Figs. 4(a), 4(c), 6(a), and 6(c)]. The other case of  $\Delta\alpha_z=15^\circ$  [Figs. 4(b) and 6(b)] corresponded to the best conditions of combustion, with small noise and a relatively high torque.

The long time scale pressure changes can have their source in the dynamics of gas exchange.<sup>17,18</sup> However, to check this possibility we need to reexamine them in future experimental series by directly measuring the content of an air/fuel mixture through an oxygen sensor. There is also the possibility that the slow pressure changes are connected with coupling of engine to measurement equipment. In this case it can be associated with an artifact caused by too small resistance of measurement wire isolation. However, it can be excluded as a leading effect as in our case we have used the same measurement equipment for all measurements.

The method using correlation entropy which we applied here differs from the symbolic treatments<sup>17,19</sup> used also for exploration of the engine dynamics by Daw *et al.*<sup>7</sup> In their paper the signal was digitized and based on the probabilities of 0 1 sequence probabilities the information Shannon entropy was estimated. In our paper we have estimated the NTS ratio by fitting coarse-grained entropy obtained from

experimental time series to a general formula of correlation entropy evaluated in the presence of noise. In our case the entropy has its dynamical meaning as a measure uncertainty of the system state.

One should also note that our present examination was limited to only one crank rotational speed 1000 rpm. Using the above-noted procedure we are now preparing systematic analysis with the other speeds for a future report.

## ACKNOWLEDGMENTS

K.U. and G.L. would like to thank Max Planck Institute for Physics of Complex Systems in Dresden for hospitality. During their stay in Dresden an important part of the data analysis was performed. K.U. has been partially supported by KBN Grant No. 2P03B03224.

- <sup>1</sup>D. Clerk, *The Gas Engine* (Longmans, London, 1886).
- <sup>2</sup>M. Wendeker, A. Niewczas, and B. Hawryluk, SAE Paper No. 00P-172, 1999.
- <sup>3</sup>J.B. Roberts, J.C. Peyton-Jones, and K.J. Landsborough, SAE Paper No. 970059, 1997.
- <sup>4</sup>Z. Hu, SAE Paper No. 961197, 1996.
- <sup>5</sup>J.B. Heywood, *Internal Combustion Engine Fundamentals* (McGraw-Hill, New York, 1988).
- <sup>6</sup>C.S. Daw, C.E.A. Finney, J.B. Green, Jr., M.B. Kennel, J.F. Thomas, and F.T. Connolly, SAE Paper No. 962086, 1996.
- <sup>7</sup>C.S. Daw, M.B. Kennel, C.E.A. Finney, and F.T. Connolly, *Phys. Rev. E* **57**, 2811 (1998).
- <sup>8</sup>M. Wendeker, J. Czarnigowski, G. Litak, and K. Szabelski, *Chaos, Solitons Fractals* **18**, 803 (2003).
- <sup>9</sup>M. Wendeker, G. Litak, J. Czarnigowski, and K. Szabelski, *Int. J. Bifurcation Chaos Appl. Sci. Eng.* (in press).
- <sup>10</sup>K. Urbanowicz and J.A. Holyst, *Phys. Rev. E* **67**, 046218 (3003).
- <sup>11</sup>S. Leonhardt, N. Müller, and R. Isermann, *IEEE/ASME Trans. Mechatron.* **4**, 235 (1999).
- <sup>12</sup>I. Antoni, J. Daniere, and F. Guillet, *J. Sound Vib.* **257**, 839 (2002).
- <sup>13</sup>T. Kamiński (unpublished).
- <sup>14</sup>H. Kantz and T. Scheiber, *Nonlinear Time Series Analysis* (Cambridge University Press, Cambridge, 1997).
- <sup>15</sup>K. Pawelzik and H.G. Schuster, *Phys. Rev. A* **35**, 481 (1987).
- <sup>16</sup>P. Grassberger and I. Procaccia, *Phys. Rev. Lett.* **50**, 346 (1983).
- <sup>17</sup>C.S. Daw, C.E.A. Finney, and M.B. Kennel, *Phys. Rev. E* **62**, 1912 (2000).
- <sup>18</sup>M. Wendeker, G. Litak, M. Krupa, *J. Vib. Control* (submitted), preprint nlin.CD/0312068.
- <sup>19</sup>C.S. Daw, C.E.A. Finney, and E.R. Tracy, *Rev. Sci. Instrum.* **74**, 915 (2003).